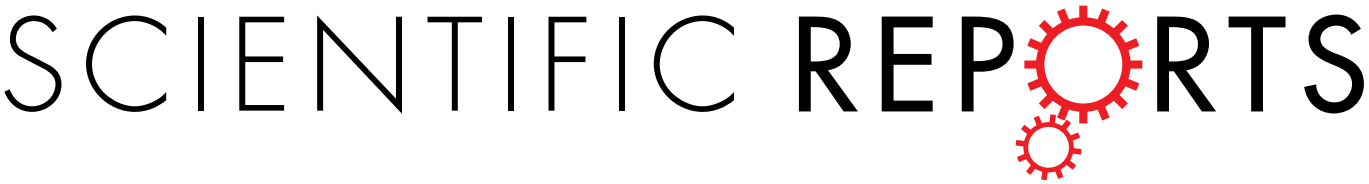

OPEN

Dielectric study on mixtures of ionic liquids

E. Thoms[1,3], P. Sippel[1], D. Reuter[1], M. Weiß[1], A. Loidl[1,2] & S. Krohns[1,2]

Received: 17 March 2017
Accepted: 3 July 2017
Published online: 07 August 2017

Ionic liquids are promising candidates for electrolytes in energy-storage systems. We demonstrate that mixing two ionic liquids allows to precisely tune their physical properties, like the dc conductivity. Moreover, these mixtures enable the gradual modification of the fragility parameter, which is believed to be a measure of the complexity of the energy landscape in supercooled liquids. The physical origin of this index is still under debate; therefore, mixing ionic liquids can provide further insights. From the chemical point of view, tuning ionic liquids via mixing is an easy and thus an economic way. For this study, we performed detailed investigations by broadband dielectric spectroscopy and differential scanning calorimetry on two mixing series of ionic liquids. One series combines an imidazole based with a pyridine based ionic liquid and the other two different anions in an imidazole based ionic liquid. The analysis of the glass-transition temperatures and the thorough evaluations of the measured dielectric permittivity and conductivity spectra reveal that the dynamics in mixtures of ionic liquids are well defined by the fractions of their parent compounds.

Ionic liquids have become one of the most popular material classes in material science[1–4] based on their versatile potential applications[5–9]. They are salts that are liquid below 100 °C and offer beneficial properties, e.g., low volatility and high electrochemical stability. This makes them ideal candidates for solvent-free electrolytes to improve many energy applications[8]. Unfortunately, the known ionic liquids do not satisfy the requirements for energy-storage technologies in terms of their ionic conductivity, which is at room temperature lower compared to organic electrolytes[10,11]. The conductivity of the electrolyte limits the power performance in energy applications, which is a key-factor for enhanced supercapacitors or batteries. Nowadays, the relatively low conductivity of ionic liquids restricts their applicability as electrolyte to some niche products[10]. However, they are regarded as 'designer solvents' because of the vast number of possible anions and cations to form an ionic liquid. A number that is further extended by the possibility to combine two or three ionic liquids via mixing[12]. There is a high possibility to design an ionic-liquid electrolyte that meets the required ionic conductivity[6,10,13]. Tuning ionic liquids via mixing is desirable, as it is more economic than altering their molecular structure[14]. Interestingly, an increased conductivity has been reported for some mixtures of ionic liquids (e.g., refs 15–17 in comparison to their parent compounds. These and similar findings suggest that unique properties are accessible via mixing ionic liquids[18]. This way of optimization seems to be restricted to only a few substances. For many mixing series the concentration is linear to the conductivity in a logarithmic scale[4]. Most of the series analyzed so far closely follow ideal mixing-laws[14,19,20], although the general picture is still unclear[4]. Niedermeyer *et al.* and Chatel *et al.* (refs 4, 18, respectively) review the topic in detail and point out the necessity for more data sets of the physical and chemical properties (e.g., conductivity) for ionic liquid mixtures. A systematic use of spectroscopic analysis is required to understand the complex intrinsic interactions and the underlying physical mechanisms[18], which are of key relevance for future applications based on mixtures of ionic liquids[18]. To the best of our knowledge, there are only a few works considering the temperature dependence of the conductivity of ionic liquid mixtures (i.e. refs 15, 17, 21–25 and solely Stoppa *et al.*[16] performed dielectric spectroscopy. In the present work, we thoroughly investigate two binary mixtures of ionic liquids using broadband dielectric spectroscopy and differential scanning calorimetry (DSC). The mixtures are analyzed regarding their glass-transition temperature (T_g), ionic conductivity and their main reorientational relaxation, as determined from the dielectric spectra via an equivalent-circuit approach. Finally, we verify the correlation of T_g and the fragility index m to the conductivity, which was found in a previous work[26]. In the first series, a two cation-based ionic liquid of 1-Butyl-3-methyl-imidazolium

[1]Experimental Physics V, Center for Electronic Correlations and Magnetism, University of Augsburg, 86135, Augsburg, Germany. [2]Institute for Materials Resource Management, University of Augsburg, 86135, Augsburg, Germany. [3]Present address: Division for Biophysics and Molecular Physics, Silesian Center for Education and Interdisciplinary Research, 75 Pulku Piechoty 1A, 41–500, Chorzow, Poland. Correspondence and requests for materials should be addressed to P.S. (email: pit.sippel@physik.uni-augsburg.de)

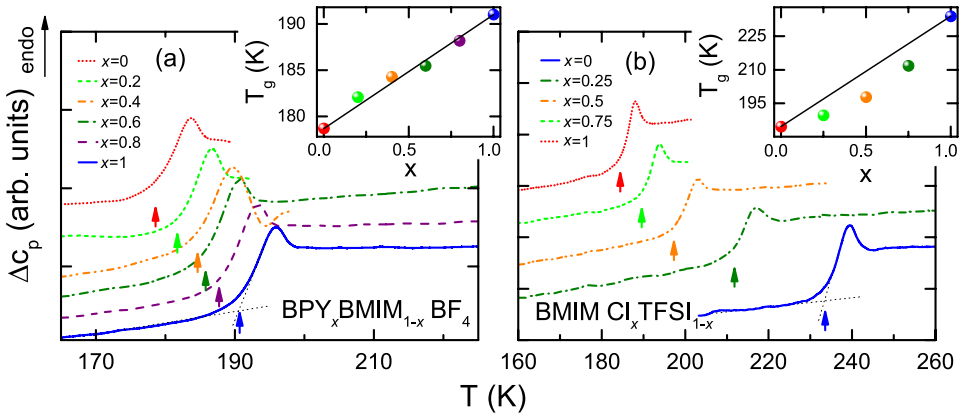

Figure 1. Shift of glass-transition temperature for two mixtures of ionic liquids. Differential Scanning Calorimetry heating traces of BPY_xBMIM_{1-x} BF_4 (**a**) with $x = 0/0.2/0.4/0.6/0.8/1.0$ and BMIM Cl_xTFSI_{1-x} (**b**) with $x = 0/0.25/0.5/0.75/1.0$ (endotherm up). The colored arrows mark the onset points used to determine T_g. The dependence of T_g on composition is shown in the insets, where the black lines indicate linear extrapolation of T_g between $x = 0$ and 1.

tetrafluoroborate (BMIM BF_4) and 1-Butylpyridinium tetrafluoroborat (BPY BF_4) is examined. For the second series a two anion-based ionic liquid of 1-Butyl-3-methyl-imidazolium bis(trifluoromethylsulfonyl)imide (BMIM TFSI) and 1-Butyl-3-methyl-imidazolium chloride (BMIM Cl) is used. Since water impurity may influence the physical properties of ionic liquids[27,28], all samples were dried prior to the measurement and the amount of water was determined via Karl Fischer titration (KFT) when possible.

Results and Discussion

Differential Scanning Calorimetry. Upon cooling, most ionic liquids can be solidified via a glass transition[26,29] as it was observed for all samples by DSC. Figure 1(a) and (b) show a magnified view of the step-like anomaly in the heat flow that is associated with the glass transition from the heating run for BPY_xBMIM_{1-x} BF_4 and BMIM Cl_xTFSI_{1-x}, respectively. The measurements were performed between 300 K and 100 K with a cooling and heating rate of 10 K/min. Prior to this measurements, all samples were dried under suitable conditions. The preparation of the samples, drying procedures and water contents are described in detail in the methods section. To determine the glass-transition temperature, the onset method is used, as depicted by the blue dotted straight lines in Fig. 1(a) and (b).

The glass-transition temperature for the pure component BPY BF_4 of the series of BPY_xBMIM_{1-x} BF_4 (Fig. 1(a)) is 191 K. When adding BMIM BF_4, T_g shifts continuously to lower temperatures as indicated by the arrows. Finally, for pure BMIM BF_4, T_g is 179 K. The inset in Fig. 1(a) illustrates the change of T_g as function of the mole fraction x of BPY_xBMIM_{1-x} BF_4. This change can be described by the line that represents the weighted average of T_g of the two pure ionic liquids, as the deviations are well below 1 K for all samples. Likewise, a glass-transition temperature between the two simple ionic liquids of a mixture has been reported in literature[22,30] and many ionic-liquid mixtures reveal a nearly linear trend of T_g with a change of concentration[14,15].

The second mixing series of BMIM Cl_xTFSI_{1-x} is shown in Fig. 1(b). BMIM Cl exhibits a T_g of 234 K and again, T_g is lowered with decreasing x. For pure BMIM TFSI we report a T_g of 185 K. The black line in the inset of Fig. 1(b) is a linear extrapolation between the glass-transition temperatures of the two constituents. However, the measured transition temperatures of the samples with $x = 0.25$, 0.5 and 0.75 show a decrease of 7, 11 and 9 K with respect to this line. Previously it was shown[28] that residual water has a huge impact on T_g of BMIM Cl. Yet considering the careful sample preparation and the trend of T_g of BMIM Cl with amount of residual water[28], we assume that water impurities cannot explain this discrepancy. Notably all glass-transition temperatures of the mixtures are below the linear extrapolation, i.e., they are closer to T_g of BMIM TFSI. This points towards a dominant influence of BMIM TFSI on the glass temperature of this mixture. A possible explanation is that due to steric reasons the impact of the huge TFSI-anion is more significant for the glass transition, than the small chloride ion of BMIM Cl. Overall, the glass-transition temperatures are all between the parent compounds.

Dielectric Spectroscopy. We have measured the dielectric response of the two mixing series BPY_xBMIM_{1-x} BF_4 with $x = 0/0.6/1.0$ and BMIM Cl_xTFSI_{1-x} with $x = 0/0.5/1.0$ in a broad frequency-range from 1 Hz to 3 GHz (for BPyBF4 the spectrum was expanded to 40 GHz) and a wide temperature range from 170 to 373 K. This range allows a thorough analysis of the conductivity and the reorientational modes in the glassy and liquid phases of these systems. The samples were dried at about 373 K for at least 16 h inside a nitrogen gas cryostat until the dielectric properties reach time-dependent constant values (not shown). This is a typical sign for no further water removal[28], suggesting stable conditions with low values of water impurities. Subsequently, the samples were measured in the same cryostat to avoid a reabsorption of water prior to the measurement. The extended measurements above 3 GHz (c.f. Fig. 2(g–i)) had to be performed in ambient atmosphere and therefore previous drying in an oven in analogy to the calorimetry measurements were performed. Unfortunately, in all cases the sample size is too small for KFT, thus the exact water content cannot be determined after the dielectric measurements. However,

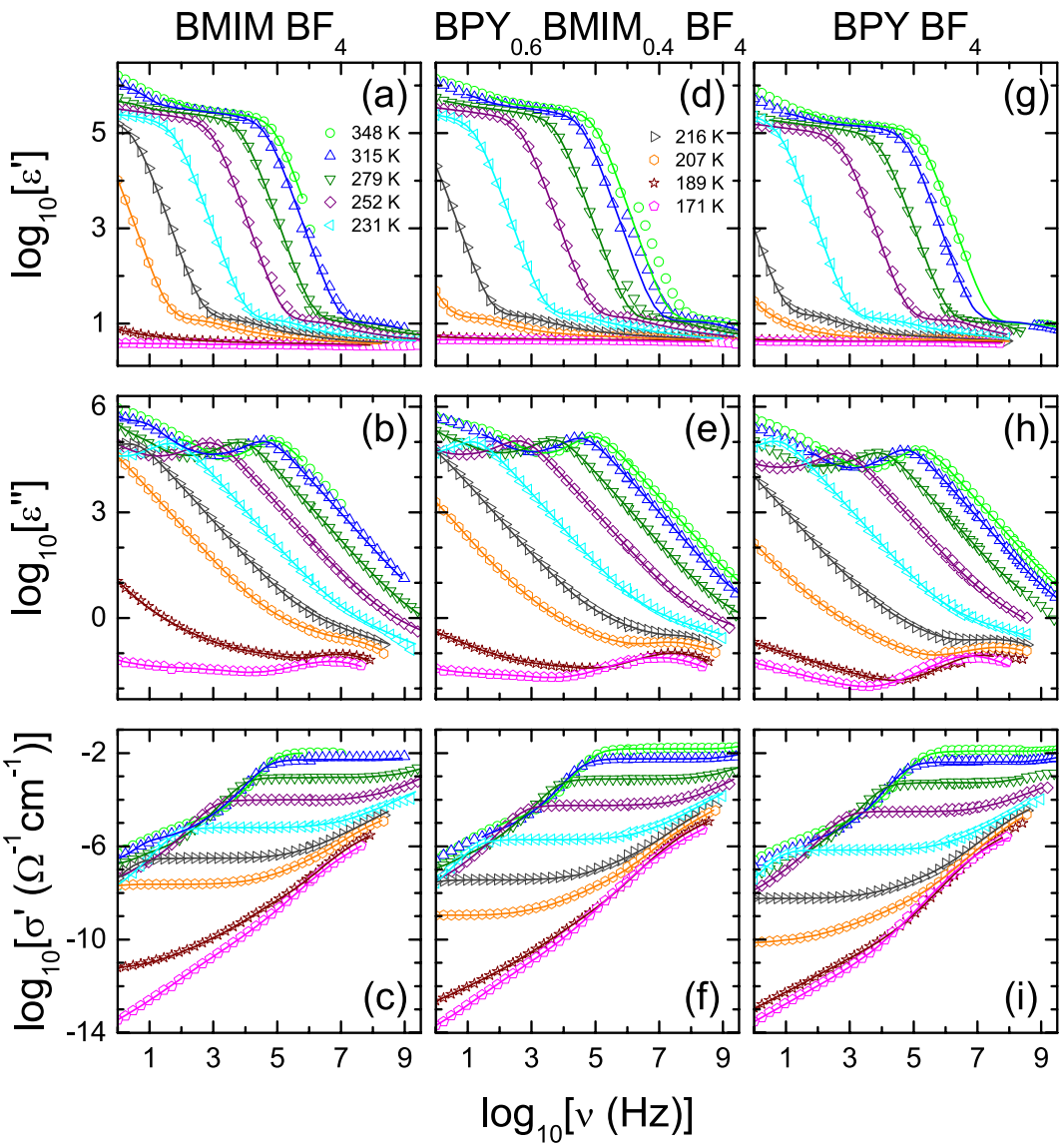

Figure 2. Dielectric spectra of ionic liquids and their mixture. Frequency dependence of permittivity ε', dielectric loss ε'' and conductivity σ' of BMIM BF_4 (**a**–**c**), $BPY_{0.6}BMIM_{0.4}$ BF_4 (**d**–**f**) and BPY BF_4 (**g**–**i**). The lines are simultaneous fits of ε' and ε'' with two distributed RC circuits[36] in series with dc conductivity and the sum of three intrinsic relaxations[37]. The temperatures for all frames are denoted in (**a**) and (**d**).

no differences between the temperature-dependent cooling and heating runs were found, suggesting a constant and low amount of water impurity. Figure 2 displays the spectra of the cooling run of the BPY_xBMIM_{1-x} BF_4 series for selected temperatures. The real ((a), (d) and (g)) and imaginary ((b), (e) and (h)) parts of the dielectric permittivity (ε' and ε'', respectively) as well as the conductivity σ' in (c), (f) and (i) are shown. The conductivity emphasizes the dc conductivity, although the information is already contained in ε'' because of $\sigma' = \omega\varepsilon_0\varepsilon''$, where ε_0 is the permittivity of free space. The rather controversially debated modulus representation (i.e., $M^* \propto 1/\varepsilon^*$), sometimes used to characterize the ionic dynamics in ion conductors[31–35] is not presented, since permittivity and conductivity allow a more direct determination of the technically relevant dc conductivity.

The spectra of Fig. 2(a) are dominated by a huge increase of $\varepsilon'(\nu)$ above 10^5 towards lower frequencies, which is typically found in many ion conductors, including ionic liquids[36,38]. This non-intrinsic effect of electrode polarization leads to a pseudo capacitance that is not an asset of the sample. It causes so-called colossal values[39] in the spectra of ε' and superimposes the intrinsic sample properties. The electrode polarization shows up as a so-called Maxwell-Wagner (MW) relaxation step in ε' (ν) that should lead to well-defined plateaus at low frequencies[37]. However, as in many ion conducting materials, no distinct plateau is approached[36]. This effect can be ascribed to the presence of several MW-relaxations or by a distribution of MW-relaxation times as discussed, e.g., in ref. 36. The MW-relaxation evolves as a step in ε' and a local maximum in ε''. It is observed in Fig. 2(b), e.g., at about 10^5 Hz for the 348 K curve and is shifting towards lower frequencies with decreasing temperature. This temperature dependence originates from an increasing sample viscosity. The high-frequency flanks of these

local maxima arise from the dc conductivity, which becomes more obvious in the conductivity representation (Fig. 2(c)) by the corresponding frequency-independent plateaus, e.g., from 1 kHz to 1 MHz for the 231 K curve. At lower frequencies, the electrode polarization leads to a decrease in conductivity, making it necessary to conduct ac-measurements to determine the dc conductivity.

At high frequencies, e.g., above 1 MHz for the 231 K curve, the conductivity in Fig. 2(c) has a pronounced frequency dependency. This indicates the presence of one or more intrinsic relaxations. The dielectric loss (Fig. 2(b)) shows signatures of a relaxational process indicated as peaks at the lowest temperatures and at elevated frequencies, e.g., around 5 MHz for the 171 K curve. The corresponding steps in the real part of the dielectric permittivity (Fig. 2(a)) are not visible at the current scaling of the spectra. Figure 2(a) reveals additional shoulders that are superimposed on the electrode polarization effect, indicating a further intrinsic relaxation with ε_s in the order of 10, e.g., above 1 kHz for the 252 K curve. The corresponding peaks in the dielectric loss (Fig. 2(b)) are covered by the dc conductivity but their high-frequency flank may cause the flattening of the spectra towards higher frequencies. This is also indicated by the increase of the conductivity at frequencies above the dc-plateau (Fig. 2(c)).

The processes described above can be analyzed in more detail by fitting the spectra simultaneously in $\varepsilon'(\nu)$ and $\varepsilon''(\nu)$ with an equivalent-circuit[37,39]. To account for the strong MW-relaxations, we used two distributed RC circuits[36,40], connected in series to the bulk response. The latter consists of a resistor representing the dc conductivity, connected in parallel to three complex capacitances that represent the intrinsic reorientational modes. In addition to the two relaxations mentioned above, at some temperatures a third process, allocated at frequencies in-between, improved the accuracy of the fit significantly. Although the whole equivalent-circuit represents the sample, only parts of the elements were needed for the fit at certain temperatures. The main reorientational mode, e.g., in Fig. 2(a) at 1 kHz for the 207 K curve, was modeled by a Cole-Davidson (CD) function[41], as often employed in glassy matter[42,43]. It is most likely caused by the reorientation of the cations[44,45]. The other relaxations were modeled by Cole-Cole functions[46]. For imidazole-based ionic liquids, a relaxation similar to the relaxational process at higher frequencies, e.g., around 5 MHz for the 171 K curve in Fig. 2(b), was discussed[44] in terms of a secondary Johari-Goldstein relaxation[47]. The Cole-Cole function is known to provide a good description for such secondary relaxations[48]. In summary, the found spectra are typical for ionic liquids and similar succession of dynamic processes were reported in several works[26,44,45,49–55].

In general, the dielectric properties of $BPY_{0.6}BMIM_{0.4}$ BF_4 and BPY BF_4, shown in Fig. 2(d–i), are quite similar to the spectra of BMIM BF_4. Again, the equivalent-circuit described above was used to analyze the dielectric behavior. For BPY BF_4, the third intrinsic process was not required to describe the experimental data. The origin of this third intrinsic relaxation is still under debate. Our results are suggesting that it is only present in imidazole-based ionic liquids. However, the relaxation is rather weak ($\Delta\varepsilon \approx 0.2$) and superimposed by stronger relaxations for the most temperatures. Thus, we cannot exclude that the third relaxation is ubiquitous for all investigated ILs.

The dielectric properties of BMIM Cl_xTFSI_{1-x} (not shown) can be well described with the same equivalent-circuit. The third intrinsic relaxation was also found in all liquids of this series and it is most pronounced for BMIM TFSI leading to $\Delta\varepsilon \approx 0.9$. For BMIM TFSI, this relaxation was attributed in ref. 44 to an intrinsic Johari-Goldstein process arising from the presence of a nonsymmetrical anion. However, for ILs with symmetric anions, e.g. BF_4, this intrinsic relaxation emerges, too. A conventional Johari-Goldstein relaxation, as discussed for $BPY_{1-x}BMIM_x$ BF_4, can explain the dielectric behavior.

For the $BPY_{1-x}BMIM_x$ BF_4 series, the dc conductivity shows a dependence on the mixting ratio x, most notably at lower temperatures. At temperatures above 279 K (cf. Fig. 2(c,f,i)) σ_{dc} reveals almost the same value when changing x. In contrast, at lower temperatures the plateau significantly diverges, e.g., at 207 K in Fig. 2(c,f,i). This implies a change in the temperature dependence of the dc conductivity based on different glass-transition temperatures of these liquids. Naturally the local maximum in ε'' (cf. Fig. 2(b,e,h)) of the MW-relaxation shifts towards lower frequencies for reduced conductivities. At lower temperatures ($T < 235$ K) the main reorientational mode (cf. Fig. 2(a) around 1 kHz for 207 K) is affected as well, which is shown in Fig. 2(d) and (g). All properties of the investigated mixture are located well between their two parent ionic liquids, which is also expected from the measurements of the glass-transition temperatures. The discussion focuses on the temperature dependence of the dc conductivity and the main reorientational mode determined from the fits of the dielectric properties for both mixing series.

Relaxation and conductivity dynamics. Fig. 3 shows the average relaxation time $\langle\tau_\alpha\rangle = \beta\tau_\alpha$ (where β is the broadening parameter of the CD function) of the main relaxation ((a) and (c)) and the dc conductivity ((b) and (d)) for both measurement series in an Arrhenius representation, as obtained by the fits described above. Both, the main relaxation time and the dc conductivity reveal the typical non-Arrhenius temperature dependence known from glass forming systems. Such behavior was reported for many ionic liquids[26,33,35,51,54,56–62]. Fits (solid lines) with the empirical Vogel-Fulcher-Tammann (VFT) law[63–66],

$$\tau = \tau_0 \exp\left[\frac{DT_{VFT}}{T - T_{VFT}}\right], \tag{1}$$

where τ_0 is the inverse attempt frequency, T_{VFT} the divergence temperature and D the so-called strength parameter[66], are most suitable to describe the obtained data. For the dc conductivity, a modified form of eq. (1) with a negative exponent and σ_0 as prefactor instead of τ_0 was used. Most commonly, the fragility index m, which is defined as the slope at T_g in the Angell plot, $\log\tau$ *vs.* T_g/T (ref. 67, is used to parameterize the deviation from Arrhenius behavior. Following Böhmer *et al.* (ref. 67), it can be calculated from the strength parameter via $m = 16 + 590/D$. The VFT-fits of $\langle\tau_\alpha\rangle$ allow to determine T_g using the empirical relation $\langle\tau_\alpha\rangle(T_g) = 100$ s. In many ionic liquids the glass-transition temperature of the ionic subsystem $\tau_\sigma(T_g) = 100$ s, derived from the modulus

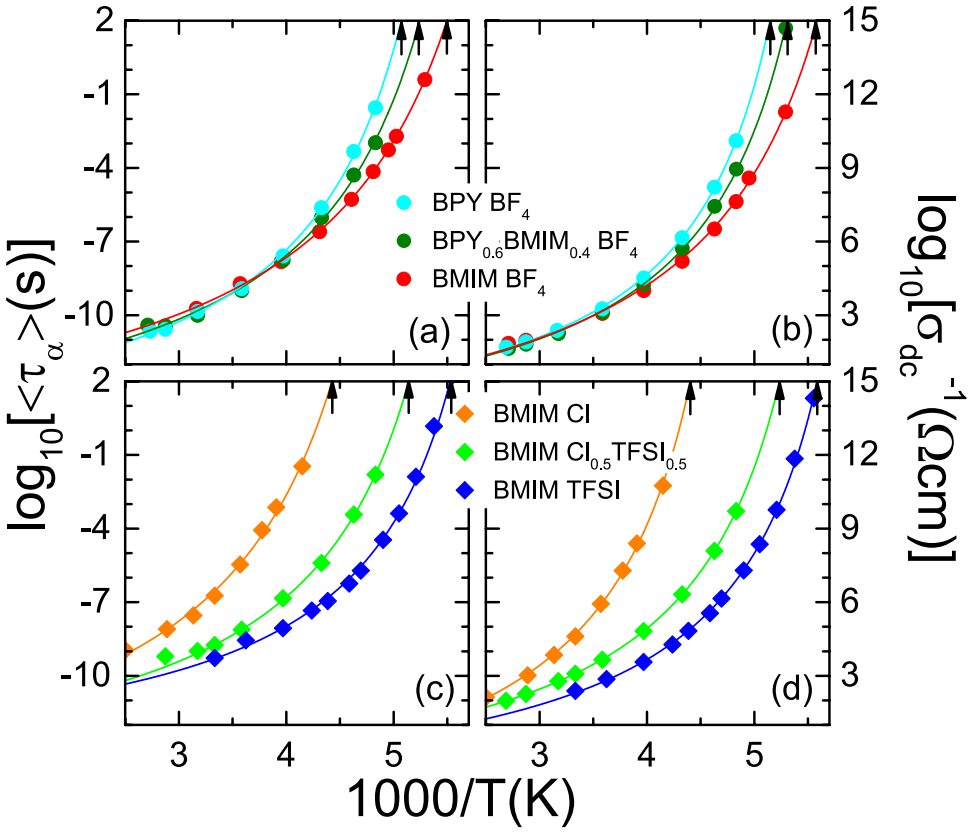

Figure 3. Temperature dependent ionic dynamics of BPY_xBMIM_{1-x} BF_4 and BMIM Cl_xTFSI_{1-x}. The relaxation times (**a**) and (**c**) and the dc-conductivities (**b**) and (**d**) are shown in an Arrhenius representation. The data are determined from the fits of the dielectric spectra. The lines are fits with the Vogel-Fulcher-Tammann-equation[63–66]. The arrows denote the glass temperatures, derived from the VFT fits at 100 s.

relaxation, reasonably matches the temperature of $\sigma_{dc} = 10^{-15}\,\Omega^{-1}\,cm^{-1}$ (ref. 26). Here, we determined T_g of the ionic subsystem from the conductivity via this relation. These two temperatures are directly evaluated by the intersection of the VFT-fit and the upper ordinates and are indicated by the black arrows (cf. Fig. 3). Generally, the main relaxation time and the dc conductivity of both parent compounds comprise the behavior of their mixtures over the whole temperature range, as illustrated by Fig. 3.

For BPY_xBMIM_{1-x} BF_4 (Fig. 3(a) and (b)), the evolution of the dc conductivity and the relaxation times reveal almost identical values above 286 K (1000/T < 3.5). Due to their different glass-transition temperatures, the curves diverge upon further cooling. The glass-transition temperatures of the main relaxational mode for BPY BF_4, $BPY_{0.6}BMIM_{0.4}$ BF_4 and BMIM BF_4 are 197, 191 and 182 K, respectively. The temperatures deduced from the conductivity are slightly (about 2 K) below. The transition temperature of the mixture is at the weighted average of T_g of the two pure parent ionic liquids, which was also evidenced by the DSC measurements. However, the absolute values are slightly above the DSC results. The highest deviation is found for pure BPY BF_4. This indicates different water content for both experiments. Another explanation is a decoupling effect of the structural glass-transition temperature derived from DSC measurements and the ionic or rotational subsystems. The rather low deviations of the other samples indicate no significant decoupling in this series.We expect, based on our previous work (ref. 26), a change in fragility due to the similar dc-conductivities at room-temperature and different glass-transition temperatures. Indeed, the fragility index *m*, determined from the conductivity, is decreasing from 117 via 111 to 93 for lower glass-transition temperatures. This mixing series is close to ideal mixing as described by Clough *et al.* in ref. 14 for their ionic liquid mixtures.

The dielectric properties of the pure ionic liquids of BMIM Cl_xTFSI_{1-x} differ even at high temperatures, as shown in Fig. 3(c) and (d). BMIM Cl exhibits the highest T_g. Its dynamics are slower than those of BMIM TFSI and the mixture. The glass-transition temperatures determined from the main relaxational mode are 181, 195 and 232 K for BMIM TFSI, BMIM $Cl_{0.5}TFSI_{0.5}$ and BMIM Cl, respectively. The glass-transition temperatures deduced from the conductivity are 179, 191 and 228 K, which is slightly lower. These values are within measurement accuracy of the DSC results and there is no decoupling in this series as well. Corresponding to the results of the DSC measurement, the mixture exhibits a T_g which is about 10 K lower than the expected T_g using the weighted average of T_g of the pure ionic liquids. In this regard, this ionic liquid mixture deviates from the ideal mixing behavior. However, the fragility index *m* of BMIM $Cl_{0.5}TFSI_{0.5}$, determined from the VFT-fit of the dc conductivity, is about 107. Interestingly, this is close to the weighted average of fragility indices of the parent compounds BMIM TFSI and BMIM Cl, being 120 and 97, respectively.

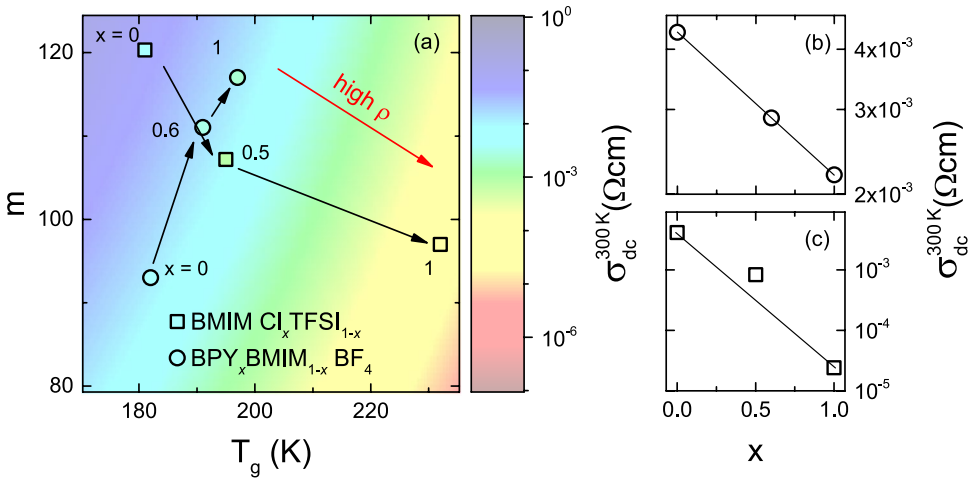

Figure 4. Fragility, glass-transition temperature and room-temperature conductivity of the mixed ionic liquids. Fragility and T_g are given in (**a**) for BPY_xBMIM_{1-x} BF_4 and BMIM Cl_xTFSI_{1-x}, as derived from the temperature dependence of the ionic dynamics. Black arrows indicate variations of x. The color-coded background (**a**) represents conductivity as a correlation of m and T_g, according to ref. 26. The symbols' color represent the measured conductivity of the samples at room temperature. Additionally room-temperature conductivity *vs*. the mole fraction x is shown for BPY_xBMIM_{1-x} BF_4 (**b**) and BMIM Cl_xTFSI_{1-x} (**c**).

Correlation of σ_{dc} with m and glass-transition temperature. Many aprotic ionic liquids exhibit a correlation of room-temperature conductivity with their T_g and fragility index[26]. This correlation is deduced from the temperature dependent dc conductivity following a VFT-law, which is dominated by these two glass-parameters. The room temperature conductivity is calculated by inserting the relaxation time of the glass-transition temperature ($\tau(T_g) = 100$ s) and the formula for the fragility index ($m = 16 + 590/D$) into the VFT-equation[26]. The conductivity derived from that formula is shown as color-coded plane in the background of Fig. 4. This illustrates the trend of the room-temperature conductivity in correlation with T_g and m. As indicated by the red arrow the conductivity decreases with increasing T_g and decreasing fragility. T_g and the fragility of both mixing series were determined from the VFT-fit of the dc conductivity, as discussed above.

The circles in Fig. 4(a) represent the results of $BPY_xBMIM_{1-x}BF_4$. The colors of the symbols, which depicts the measured dc conductivity at room temperature, show almost identical values. The connecting black arrows that indicate variations of x, are almost parallel to a line of constant conductivity given by the $\sigma(T_g,m)$ relation, following a trajectory of isoconductivity. That means, changes of the conductivity from the reduced T_g are compensated by the fragility, as it is expected from the Arrhenius plot in Fig. 3. The squares represent BMIM Cl_xTFSI_{1-x}, which shows an decreasing conductivity for increasing x. Both the decreased fragility index and the increased T_g diminish the conductivity. The variation of x results in conductivities almost parallel to the gradient of the colored plane. In summary, the trend of the dc-conductivities is well described by the colored plane, allowing to characterize the conductivity of the ionic liquids mixtures via the fragility index and T_g. Figure 4(b) and (c) show a plot of the room-temperature conductivity as a function of x. The line represents a linear change of the conductivity on a logarithmic scale, as expected for an ideal mixture[4]. For BPY_xBMIM_{1-x} BF_4 the mixture with $x = 0.6$ meets the line as predicted for an ideal mixture. Whereas, the dc conductivity at room temperature for BMIM $Cl_{0.5}TFSI_{0.5}$ is raised compared to this line. Most likely, this increase is based on the reduced glass temperature, as discussed above.

Summary

The ionic liquids BPY BF_4 and BMIM BF_4 display ideal mixing, as their glass-transition temperatures and conductivities show a linear dependence on the composition. We provide glass-transition temperatures revealed by DSC experiments and by dielectric spectroscopy of $BPY_{0.6}BMIM_{0.4}$ BF_4, corresponding to the weighted average of their parent compounds. In addition, the dielectric properties of the mixture mimic those of the parent compounds, exhibiting relaxational dynamics and conductivities exactly between them. Interestingly, even the fragility index of the mixture, which can be regarded as a measure for the complexity of the energy landscape, is well between the parent compounds. The dielectric properties of BMIM Cl_xTFSI_{1-x} suggest a linear behavior of the fragility when mixing the two parent compounds. This indicates the possibility to design ternary ionic liquids with precisely defined fragilities, opening a way to gain further insights on a quantity whose physical origin is still unclear. However, the linearity of the fragility when mixing ionic liquids has to be evidenced in further compounds. In contrast, the glass-transition temperatures of the mixtures deviate about 10 K from their expected value, which is obtained by the weighted average of T_g of the pure ionic liquids. It is still unclear if the strong molecular difference of the anions is the reason. The relaxational dynamics and dc-conductivities of all investigated mixtures studied in this work are between the parent ionic liquids. This enables a simple route to tune, e.g., the conductivity as well as other physical properties of ionic liquids. Particularly, this way to modify the properties of ionic liquids is not only very precise, but also very economic compared to a functional design of new anion cation pairs[14]. Our work on two ionic liquid mixture series gains further insights, especially it relates the dielectric properties to the concentration.

Methods

Sample preparation. The ILs were purchased from IoLiTec with a purity of 99%. The mixtures were prepared by blending the two neat ILs in the appropriate mass ratio. To minimize water content, all samples were dried in N_2-gas or vacuum at elevated temperatures for at least 16 hours prior to the measurements. The water content of BPY_xBMIM_{1-x} BF_4 was determined using coulometric KFT after drying but before to the DSC measurements. The mixing series exhibits less than 0.3 mol% residual water for all samples: BMIM BF_4 0.23 mol%, $BPY_{0.6}BMIM_{0.4}$ BF_4 0.25 mol% and BPY BF_4 0.27 mol%. The high viscosity and hygroscopic nature of the samples of the BMIM Cl_xTFSI_{1-x} series hampered reliable KFT results. All samples of this mixing series were dried under identical conditions, i.e., for 24 h in nitrogen atmosphere at 373 K and for 48 h in reduced pressure at 353 K. Subsequently, the samples were sealed into the DSC aluminum pans in dried N_2-atmosphere. Comparing the measured T_g with previous results[27] the water content of these samples can be determined to be significant less than 1 mol%. For the dielectric measurements <3 GHz all samples were dried already in the employed cryostats, due to the small sample size no water content can be reported. The expanded spectra up to 40 GHz for BPY BF_4 was recorded in ambient atmosphere; thus the sample was dried separately, similarly as for the calorimetry measurements.

Thermal measurements. For the DSC measurements a DSC 8500 (Perkin Elmer) was used. The samples were cooled to 100 K and subsequently heated back to room temperature at 10 K/min. Aluminum pans, which were hermetically sealed after filling in the sample, were used for all measurements. The glass-transition temperatures were taken at the onset of the transition steps in the heating traces.

Dielectric measurements. The complex permittivity $\varepsilon^* = \varepsilon' - i\varepsilon''$ and the real part of the conductivity σ' at frequencies $1\,Hz \leq \nu \leq 1\,MHz$ were determined using a frequency-response analyzer (Novocontrol alpha-Analyzer) and at $1\,MHz \leq \nu \leq 3\,GHz$ employing a coaxial reflection impedance analyzer (Agilent E4991A or Keysight E4991B). All samples were measured in steel-plate capacitors. For sample cooling between 170 and 370 K, a Novocontrol Quatro Cryosystem was utilized. For BPY BF_4, the spectrum was additionally expanded to 40 GHz using a coaxial reflection measurement with an open-ended sensor (Agilent E8363B PNA Series Network Analyzer with 85070E Dielecric Probe Kit). Sample heating from 300 to 370 K was done by an Eppendorf Thermomixer Comfort with an additional external temperature sensor.

References

1. Endres, F. & Abedin, S. Z. E. Air and water stable ionic liquids in physical chemistry. *Phys. Chem. Chem. Phys.* **8**, 2101–2116 (2006).
2. Rogers, R. D., Zhang, S. J. & Wang, J. J. Preface: An international look at ionic liquids. *Sci. China Chem.* **55**, 1475–1477 (2012).
3. Hallett, J. P. & Welton, T. Room-Temperature Ionic Liquids: Solvents for Synthesis and Catalysis. 2. *Chem. Rev.* **111**, 3508–3576 (2011).
4. Niedermeyer, H., Hallett, J. P., Villar-Garcia, I. J., Hunt, P. A. & Welton, T. Mixtures of ionic liquids. *Chem. Soc. Rev.* **41**, 7780–7802 (2012).
5. Rogers, R. D. & Seddon, K. R. Ionic liquids - Solvents of the future? *Sci.* **302**, 792–793 (2003).
6. Weingärtner, H. Understanding ionic liquids at the molecular level: facts, problems, and controversies. *Angew. Chem. Int. Ed.* **47**, 654–670 (2008).
7. Armand, M., Endres, F., MacFarlane, D. R., Ohno, H. & Scrosati, B. Ionic-liquid materials for the electrochemical challenges of the future. *Nat. Mater.* **8**, 621–629 (2009).
8. MacFarlane, D. R. *et al*. Energy applications of ionic liquids. *Energy Environ. Sci.* **7**, 232–250 (2014).
9. Lin, M.-C. *et al*. An ultrafast rechargeable aluminium-ion battery. *Nature* **520**, 325–328 (2015).
10. Simon, P. & Gogotsi, Y. Materials for electrochemical capacitors. *Nat. Mater.* **7**, 845–854 (2008).
11. Beguin, F., Presser, V., Balducci, A. & Frackowiak, E. Carbons and electrolytes for advanced supercapacitors. *Adv. Mater.* **26**, 2219–2251 (2014).
12. Seddon, K. R. Ionic liquids: designer solvents for green synthesis. *Chem. Eng.* **720**, 33–35 (2002).
13. Chiappe, C. & Pieraccini, D. Ionic liquids: solvent properties and organic reactivity. *J. Phys. Org. Chem.* **18**, 275–297 (2005).
14. Clough, M. T. *et al*. A physicochemical investigation of ionic liquid mixtures. *Chem. Sci.* **6**, 1101–1114 (2015).
15. Every, H., Bishop, A. G., Forsyth, M. & MacFarlane, D. R. Ion diffusion in molten salt mixtures. *Electrochim. Acta* **45**, 1279–1284 (2000).
16. Stoppa, A., Buchner, R. & Hefter, G. How ideal are binary mixtures of room-temperature ionic liquids? *J. Mol. Liq.* **152**, 46–51 (2010).
17. Taige, M., Hilbert, D. & Schubert, T. J. S. Mixtures of Ionic Liquids as Possible Electrolytes for Lithium Ion Batteries. *Z. Phys. Chem.* **226**, 129–139 (2012).
18. Chatel, G., Pereira, J. F. B., Debbeti, V., Wang, H. & Rogers, R. D. Mixing ionic liquids - "simple mixtures" or "double salts"? *Green Chem.* **16**, 2051–2083 (2014).
19. Navia, P., Troncoso, J. & Romani, L. Excess magnitudes for ionic liquid binary mixtures with a common ion. *J. Chem. Eng. Data* **52**, 1369–1374 (2007).
20. Navia, P., Troncoso, J. & Romani, L. Viscosities for ionic liquid binary mixtures with a common ion. *J. Solution Chem.* **37**, 677–688 (2008).
21. Egashira, M., Nakagawa, M., Watanabe, L., Okada, S. & Yamaki, J. I. Cyano-containing quaternary ammonium-based ionic liquid as a 'co-solvent' for lithium battery electrolyte. *J. Power Sources* **146**, 685–688 (2005).
22. Castiglione, F. *et al*. Blending ionic liquids: how physico-chemical properties change. *Phys. Chem. Chem. Phys.* **12**, 1784–1792 (2010).
23. Scheers, J. *et al*. Ionic liquids and oligomer electrolytes based on the $B(CN)_4^-$ anion; ion association, physical and electrochemical properties. *Phys. Chem. Chem. Phys.* **13**, 14953–14959 (2011).
24. Kunze, M., Jeong, S., Appetecchi, G. B. & Passerini, S. Mixtures of ionic liquids for low temperature electrolytes. *Electrochim. Acta* **60**, 69–74 (2012).
25. Montanino, M. *et al*. Physical and electrochemical properties of binary ionic liquid mixtures: (1-x) $PYR_{14}TFSI$-(x) $PYR_{14}IM_{14}$. *Electrochim. Acta* **60**, 163–169 (2012).
26. Sippel, P., Lunkenheimer, P., Krohns, S., Thoms, E. & Loidl, A. Importance of liquid fragility for energy applications of ionic liquids. *Sci. Rep.* **5**, 13922 (2015).

27. Seddon, K. R., Stark, A. & Torres, M. J. Influence of chloride, water and organic solvents on the physical properties of ionic liquids. *Pure Appl. Chem.* **72**, 2275–2287 (2000).
28. Sippel, P. *et al*. Impact of water on the charge transport of a glass-forming ionic liquid. *J. Mol. Liq.* **223**, 635–642 (2016).
29. Holbrey, J. D. & Rogers, R. D. Physiochemical Properties of Ionic Liquids: Melting Points and Phase Diagrams in *Ionic Liquids in Synthesis vol. 1* (eds. Wasserscheid, P. & Welton, T.) 57–72 (Wiley, Weiheim, 2008).
30. Kunze, M., Jeong, S., Paillard, E., Winter, M. & Passerini, S. Melting Behavior of Pyrrolidinium-Based Ionic Liquids and Their Binary Mixtures. *J. Phys. Chem. C* **114**, 12364–12369 (2010).
31. Macedo, P. B., Moynihan, C. T. & Bose, R. The role of ionic diffusion in polarisation in vitreous ionic conductors. *Phys. Chem. Glasses* **13**, 171–179 (1972).
32. Hodge, I. M., Ngai, K. L. & Moynihan, C. T. Comments on the electric modulus function. *J. Non-Cryst. Solids* **351**, 104–115 (2005).
33. Rivera, A., Brodin, A., Pugachev, A. & Rössler, E. A. Orientational and translational dynamics in room temperature ionic liquids. *J. Chem. Phys.* **126**, 114503 (2007).
34. Sangoro, J. R. & Kremer, F. Charge transport and glassy dynamics in ionic liquids. *Acc. Chem. Res.* **45**, 525–531 (2011).
35. Wojnarowska, Z. & Paluch, M. Recent progress on dielectric properties of protic ionic liquids. *J. Phys. Condens. Matter* **27**, 073202 (2015).
36. Emmert, S. *et al*. Electrode polarization effects in broadband dielectric spectroscopy. *Eur. Phys. J. B* **83**, 157–165 (2011).
37. Lunkenheimer, P. *et al*. Colossal dielectric constants in transition-metal oxides. *Eur. Phys. J. Special Topics* **180**, 61–89 (2010).
38. Macdonald, J. R. Comparison and discussion of some theories of the equilibrium double layer in liquid electrolytes. *J. Electroanal. Chem.* **223**, 1–23 (1987).
39. Lunkenheimer, P. *et al*. Origin of apparent colossal dielectric constants. *Phys. Rev. B* **66**, 052105 (2002).
40. Lunkenheimer, P., Knebel, G., Pimenov, A., Emelchenko, G. A. & Loidl, A. Dc and ac conductivity of La2CuO$_{4+\delta}$. *Z. Phys. B Condens. Matter* **99**, 507–516 (1996).
41. Davidson, D. W. & Cole, R. H. Dielectric relaxation in glycerol, propylene glycol, and n-propanol. *J. Chem. Phys.* **19**, 1484–1490 (1951).
42. Lunkenheimer, P., Schneider, U., Brand, R. & Loidl, A. Glassy dynamics. *Contemp. Phys.* **41**, 15–36 (2000).
43. Kremer, F. & Schönhals A. Analysis of Dielectric Spectra. In *Broadband Dielectric Spectroscopy* (eds. Kremer, F. & Schönhals, A.) 59–98 (Springer, Berlin, 2009).
44. Rivera, A. & Rössler, E. A. Evidence of secondary relaxations in the dielectric spectra of ionic liquids. *Phys. Rev. B* **73**, 212201 (2006).
45. Nakamura, K. & Shikata, T. Systematic dielectric and NMR study of the ionic liquid 1-alkyl-3-methyl imidazolium. *ChemPhysChem* **11**, 285–294 (2010).
46. Cole, K. S. & Cole, R. H. Dispersion and absorption in dielectrics I. Alternating current characteristics. *J. Chem. Phys.* **9**, 341–351 (1941).
47. Johari, G. P. & Goldstein, M. Viscous liquids and the glass transition. II. Secondary relaxations in glasses of rigid molecules. *J. Chem. Phys.* **53**, 2372–2388 (1970).
48. Kastner, S., Köhler, M., Goncharov, Y., Lunkenheimer, P. & Loidl, A. High-frequency dynamics of type-B glass formers investigated by broadband dielectric spectroscopy. *J. Non-Cryst. Solids* **357**, 510–514 (2011).
49. Weingärtner, H., Knocks, A., Schrader, W. & Kaatze, U. Dielectric spectroscopy of the room temperature molten salt ethylammonium nitrate. *J. Phys. Chem A* **105**, 8646–8650 (2001).
50. Stoppa, A. *et al*. Interactions and dynamics in ionic liquids. *J. Phys. Chem. B* **112**, 4854–4858 (2008).
51. Sangoro, J. *et al*. Electrical conductivity and translational diffusion in the 1-butyl-3-methylimidazolium tetrafluoroborate ionic liquid. *J. Chem. Phys.* **128**, 214509 (2008).
52. Buchner, R. & Hefter, G. Interactions and dynamics in electrolyte solutions by dielectric spectroscopy. *Phys. Chem. Chem. Phys.* **11**, 8984–8999 (2009).
53. Hunger, J., Stoppa, A., Schrödle, S., Hefter, G. & Buchner, R. Temperature dependence of the dielectric properties and dynamics of ionic liquids. *ChemPhysChem* **10**, 723–733 (2009).
54. Krause, C., Sangoro, J. R., Iacob, C. & Kremer, F. Charge transport and dipolar relaxations in imidazolium-based ionic liquids. *J. Phys. Chem. B* **114**, 382–386 (2010).
55. Weingärtner, H. The static dielectric permittivity of ionic liquids. *J. Mol. Liq.* **192**, 185–190 (2014).
56. Angell, C. A., Ansari, Y. & Zhao, Z. Ionic Liquids: Past, present and future. *Faraday Discuss.* **154**, 9–27 (2012).
57. Xu, W., Cooper, E. I. & Angell, C. A. Ionic liquids: Ion mobilities, glass temperatures, and fragilities. *J. Phys. Chem. B* **107**, 6170–6178 (2003).
58. Ueno, K., Zhao, T., Watanabe, M. & Angell, C. A. Protic ionic liquids based on decahydroisoquinoline: Lost superfragility and ionicity-fragility correlation. *Phys. Chem. B* **116**, 63–70 (2012).
59. Sangoro, J. R. *et al*. Charge transport and mass transport in imidazolium-based ionic liquids. *Phys. Rev. E* **77**, 051202 (2008).
60. Sangoro, J. R., Iacob, C., Serghei, A., Friedrich, C. & Kremer, F. Universal scaling of charge transport in glass-forming ionic liquids. *Phys. Chem. Chem. Phys.* **11**, 913–916 (2008).
61. Leys, J. *et al*. Temperature dependence of the electrical conductivity of imidazolium ionic liquids. *J. Chem. Phys.* **128**, 064509 (2008).
62. Leys, J. *et al*. Influence of the anion on the electrical conductivity and glass formation of 1-butyl-3-methylimidazolium ionic liquids. *J. Chem. Phys.* **133**, 034503 (2010).
63. Vogel, H. The law of the relationship between viscosity of liquids and the temperature. *Phys. Z* **22**, 645–646 (1921).
64. Fulcher, G. S. Analysis of recent measurements of the viscosity of glasses. *J. Am. Ceram. Soc.* **8**, 339–355 (1925).
65. Tammann, G. & Hesse, W. Die Abhängigkeit der Viscosität von der Temperatur bei unterkühlten Flüssigkeiten. *Z. Anorg. Allg. Chem.* **156**, 245–257 (1926).
66. Angell, C. A. *Strong and fragile liquids in Relaxations in Complex Systems* (eds. Ngai, K. L. & Wright, G. B.) 3–11 (NRL, Washington DC, 1985).
67. Böhmer, R., Ngai, K. L., Angell, C. A. & Plazek, D. J. Nonexponential relaxations in strong and fragile glass formers. *J. Chem. Phys.* **99**, 4201–4209 (1993).

Acknowledgements

We thank M. Aumüller and M. Weiss for performing parts of the dielectric measurements and parts of the DSC measurements. This work was supported by the BMBF via ENREKON 03EK3015 and by the Bavarian graduate school "Resource strategy concepts for sustainable energy systems" of the Institute of Materials Resource Management (MRM) of the University of Augsburg.

Author Contributions

P.S. and S.K. initiated the research. S.K. supervised the project. D.R. and M.W. performed the DSC and E.T. the dielectric measurements. P.S. and S.K. wrote the paper with contributions from E.T. and A.L. All authors discussed the results and commented on the manuscript.

Additional Information

Competing Interests: The authors declare that they have no competing interests.

Publisher's note: Springer Nature remains neutral with regard to jurisdictional claims in published maps and institutional affiliations.